

Order-disorder of Fe³⁺ ions over the tetrahedral positions in albite

IVAN PETROV, FU YUDE,* L. V. BERSHOV,* S. S. HAFNER, HERBERT KROLL*

Institute of Mineralogy, University of Marburg, Meerweinstrasse, 3550 Marburg, West Germany

ABSTRACT

The electron paramagnetic resonance (EPR) spectrum of Fe³⁺ in natural and heat-treated single crystals of albite was studied at X-band frequencies. Heat treatments were carried out between 500 and 850 °C under hydrothermal conditions. The EPR spectra were measured for B parallel to c* before and after heat treatment. The g values of the five fine-structure lines of Fe³⁺ at g_{eff} = 19.3, 4.8, 3.3, 2.3, and 1.3 (crystallographic c* parallel to external magnetic field) remained unchanged, but a significant line broadening was observed that increased with increasing Al,Si disorder. It is concluded that Fe³⁺ is located at the tetrahedral T1(O) position of Al³⁺ in low albite and does not participate in the Al,Si exchange among T sites within the range of temperatures studied. The line broadening is primarily due to increasing Al,Si disorder at adjacent Fe³⁺ sites in albite and can be correlated with observed changes in the lattice constants of the crystals. In crystals with more Al,Si disordering, the Fe³⁺ lines became exceedingly broad.

INTRODUCTION

The distribution of Al and Si over the four nonequivalent tetrahedral positions T1(O), T1(m), T2(O), and T2(m) in albite NaAlSi₃O₈ (space group C1) has been studied for many years. Natural albites from igneous and metamorphic rocks are generally well ordered, Al occupying the T1(O) position and Si being located at T1(m), T2(O), and T2(m). This structural state is designated low albite. After heat treatment at temperatures above ~650 °C, the distribution of Al and Si becomes partially disordered over all four tetrahedral positions, eventually yielding high albite. The degree of disorder increases with increasing temperature until at 980 °C, high albite inverts to monalbite (C2/m). Upon quenching, monalbite transforms by a displacive mechanism to metastable analbite (C1).

At present, very little information is available concerning the site distribution of foreign atoms substituted in minor amounts for Al or Si on tetrahedral sites. Probably the most abundant minor element in albite from terrestrial rocks is Fe³⁺ and this is commonly present at levels of ~0.1 wt%. Fe³⁺ occurs in albite as a paramagnetic center that can be studied by electron paramagnetic resonance (EPR). EPR spectra of Fe³⁺ in albite were described first by Marfunin et al. (1967) and later by Gaité and Michoulier (1970) and Matyash et al. (1981). Subsequently, Michoulier and Gaité (1972) studied the interaction of Fe³⁺ with the crystal field at its site up to fourth order. The g tensor and the B_n^m terms of the electrostatic

interaction tensor of Fe³⁺ in albite are quite well known, therefore.

In the present work (cf. also Fu et al., 1987), Fe³⁺ EPR spectra of single crystals of natural low albite were studied after heat treatment at temperatures between 500 and 850 °C with run durations of between 1 and 7 d. The aim was to investigate the kinetics of the Fe³⁺ exchange among the T sites.

EXPERIMENTAL DETAILS

Samples

The crystals used for the experiments were from Amelia Court House, Virginia, U.S.A. They were untwinned, optically transparent, quite homogeneous, and colorless. The dimensions of single-crystal fragments cut for EPR experiments were about 3 × 4 × 5 mm. The composition of Amelia albite includes approximately 0–2 mol% anorthite and 0.01–0.03 Fe pfu (cf. Deer et al., 1963).

Heat treatments

Single crystals were heated in an autoclave under hydrothermal conditions between 500 and 800 °C at a pressure of 1 kbar and at 850 °C at 0.5 kbar. Annealing times varied between 24 and 186 h. The crystals were cleaned in acetone and sealed subsequently in Au capsules with 0.1 mL H₂O. The seals of the Au capsules were tested 5, 15, and 55 min after beginning the run and again at the end. The autoclave was cooled rapidly to room temperature by blowing air onto it for 15–20 min. The shape of the crystals was generally unchanged after heating.

Electron paramagnetic resonance (EPR)

EPR spectra of single crystals were recorded at room temperature at X-band frequencies of about 9.5 GHz with a Varian E-line spectrometer using 100-kHz modulation.

* Present addresses: (Yude) Institute of Geochemistry, Academia Sinica, Guiyang, Guizhou Province, China; (Bershov) IGEM, Academy of Sciences of USSR, Moscow 109017, USSR; (Kroll) Institut für Mineralogie der Universität Münster, Corrensstrasse 24, 4400 Münster, West Germany.

The observed EPR signals were labeled by their effective g values, g_{eff} , which are defined by the relation,

$$h\nu = g_{\text{eff}}\beta\mathbf{B}.$$

Here, \mathbf{B} is the external magnetic field at which the EPR signal appears, ν is the microwave frequency used, β is the Bohr magneton, and h is Planck's constant. \mathbf{B} was varied between 0 and 1 T. The resonance frequency was determined by a frequency counter, and the magnetic field was calibrated using proton nuclear magnetic resonance. The single crystals were aligned on a goniometer in the cavity of the spectrometer. For all spectra evaluated quantitatively, \mathbf{B} was parallel to the crystal axis c^* and perpendicular to the crystal axis a . For testing the conditions of resonance generally, a synthetic single crystal of ruby containing 0.025 wt% Cr was used as a standard for intensity. The crystal was placed in a fixed position in the cavity, and the spectra of the ruby and the albite crystal were recorded simultaneously.

X-ray diffraction

X-ray diffraction data were collected for unheated and heated powder samples using a Guinier-Jagodzinski camera equipped with a Johansson-type Ge-monochromator ($\text{CuK}\alpha_1$ radiation). Spec-pure Si (SRM 640 A) was chosen as the internal standard. The reflections were measured using a high-precision ruler and a zoom-binocular. The mean error in reading is estimated to be ± 0.02 mm, which corresponds to $\pm 0.01^\circ 2\theta$. Systematic errors were corrected by a sequence of straight lines through the zero point and standard data points. The charts of Bambauer et al. (1967) and Kroll et al. (1986) were used to index the low-angle reflections, and the least-squares refinement program of Burnham (1962) was used to refine the lattice parameters. From these, the full powder pattern was calculated and the indexing completed. Line coincidences have been carefully avoided. The results are listed in Table 1.

RESULTS

The X-band EPR spectrum of Fe³⁺ in natural, ordered low albite consists of five fine-structure lines with widths of about 50 G, as shown in Figure 1. That line width is typical for ordered microcline and albite (Gaite and Michoulier, 1970). It increases with increasing Al,Si disorder; it was found to be 150–200 G, for example, for

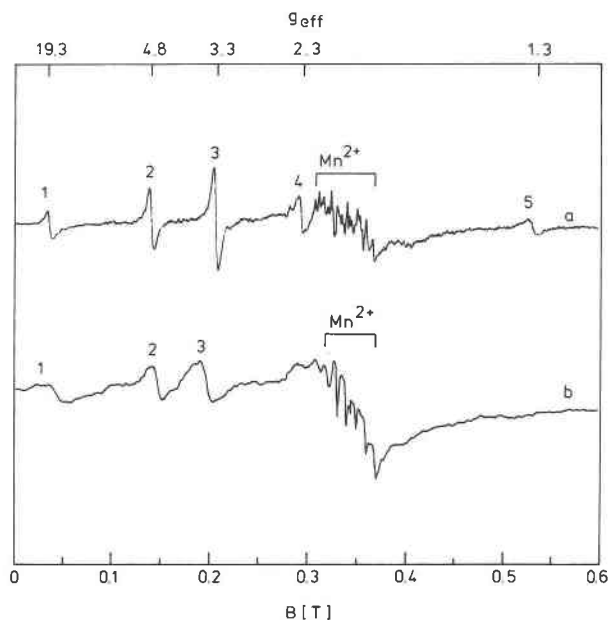


Fig. 1. EPR spectrum (X-band) of an untwinned albite single crystal from Amelia at 295 K, $\nu = 9.4465$ GHz; c^* parallel to \mathbf{B} . (a) natural crystal, (b) crystal heated at 800 °C and 1 kbar for 90 h. The signals 1, 2, 3, 4, and 5 are assigned to Fe³⁺ at the crystallographic position T1(O). The additional sextet in the region of $g_{\text{eff}} = 2$ is due to Mn²⁺. The additional very broad line between $g = 1.8$ and $g = 2.5$ in spectrum b is probably due to spin-spin interaction of iron oxide particles and/or to Fe clusters at defect positions.

sanidine (Petrov and Hafner, 1988). Highly perfect synthetic quartz or forsterite crystals may have much smaller line widths (2–3 G). Their resonance fields depend on the orientation of the crystal with respect to the applied magnetic field \mathbf{B} . The Hamiltonian of the spin interaction with the crystal field was evaluated by Michoulier and Gaite (1972), including terms of second and fourth order. The orientation c^* parallel to \mathbf{B} ($\perp a$), as used in this study, does not correspond to a special orientation, since none of the principal axes of the g tensor are then parallel to \mathbf{B} . However, for this kinetic study it was considered more important that the spectra from different samples could be compared precisely with respect to some well-defined crystallographic reference axis. This orientation

TABLE 1. Line width ΔB and cell dimensions of natural and heated albite

Sample number	T (°C)	P (kbar)	Heating time (h)	ΔB $10^{-4} T$	a (Å)	b (Å)	c (Å)	α (°)	β (°)	γ (°)	V (Å ³)	Number of (hkl) reflections
1	25	—	—	50	8.1449(4)	12.7906(3)	7.1608(4)	94.225(3)	116.582(2)	87.708(2)	665.30(7)	97
2	700	1.0	144	60	8.1438(5)	12.7921(5)	7.1586(4)	94.235(4)	116.581(3)	87.752(3)	665.10(8)	97
3	800	1.0	24	75	8.1484(6)	12.7999(7)	7.1546(4)	94.209(6)	116.571(4)	87.942(4)	665.39(9)	78
4	800	1.0	186	175	8.1509(5)	12.8093(5)	7.1465(4)	94.123(4)	116.553(3)	88.349(4)	665.72(9)	82
5	850	0.5	120	230	8.1585(5)	12.8303(7)	7.1345(4)	93.945(5)	116.516(3)	88.924(5)	666.61(9)	68

Note: Standard deviations are given in parentheses and refer to the last decimal place.

TABLE 2. Al occupancies t_{1o} , t_{1m} , t_{2o} , and t_{2m} of the respective four tetrahedral positions T1(O), T1(m), T2(O), and T2(m)

No.	t_{1o}	t_{1m}	$t_{2o} = t_{2m}$	$t_{1o} + t_{1m}$
1	1.00	0.00	0.00	1.00
2	0.98	0.01	0.01	0.99
3	0.92	0.02	0.02	0.94
4	0.81	0.07	0.06	0.88
5	0.64	0.13	0.12	0.77

Note: t values calculated from Eqns. 6 and 12 of Kroll and Ribbe (1987). The numbers 1 to 5 refer to the sample numbers and heat treatments given in Table 1. The site occupancy t^{Si} of Si is $t^{\text{Si}} = 1 - t^{\text{Al}}$.

can easily be reproduced because of the presence of (001) and (010) cleavage planes, which were always observed in our crystals. The values $g_{\text{eff}} = 19.3, 4.8, 3.3, 2.3$, and 1.3 refer to that orientation. No measurements at frequencies of the Q-band were carried out.

In addition to the five relatively sharp Fe³⁺ signals, a sextet near $g = 2$ was detected (Fig. 1) that is typical of the six hyperfine transitions of Mn²⁺ ($S = 5/2, I = 5/2$) most probably located at the Na⁺ position. To our knowledge, this sextet has not yet been described for albite. It was not studied further.

The broad line between $g_{\text{eff}} \approx 1.8$ and $g_{\text{eff}} \approx 2.5$, superimposed by the hyperfine sextet of Mn²⁺ is interpreted as resulting from spin-spin interaction of iron oxide and/or hydroxide particles, or Fe³⁺-O-Fe³⁺ clusters (cf. Griscom, 1980; Bart et al., 1982; Calas and Petiau, 1983). Mineeva et al. (1984) found similarly broad lines in the same region in the spectra of natural silicate glasses. They interpreted the lines as due to particles smaller than 10 nm that had "hematite"- and "magnetite"-like structures. Friebele et al. (1971) also observed broad lines at $g \approx 2$ in iron phosphorus glass doped with varying amounts of Fe³⁺ and Fe²⁺ ions. They ascribed those lines to antiferromagnetically coupled Fe³⁺-Fe²⁺ pairs. After heat treatment of the glass, the intensity of the line increased significantly due to exsolved Fe³⁺-rich crystallites that showed antiferromagnetic alignment of the Fe³⁺ ions.

No significant change could be observed in the EPR spectrum after heating a crystal at 500 °C for 120 h. Heating at 700, 800, and 850 °C, however, produced systematic broadening of the Fe³⁺ lines, though the position of the lines, i.e., the values of g_{eff} , remained almost unchanged. The spectrum of a crystal heated at 800 °C for 90 h is also shown in Figure 1 and may be compared to that of the original, unheated crystal.

Systematic changes in line width with annealing time were observed for all five lines in spectra from a crystal heated at 800 °C for various times of up to 186 h. The same crystal (no. 4) was used in these experiments, and its shape did not change. The variation in line width, ΔB , of the most intense line (no. 3 in Fig. 1) is illustrated in Figure 2a, where line width ΔB and relative line intensity h are also defined. In general, the recorded line shapes represent first derivatives of the resonant absorption. It should be noted, however, that, because of broadening,

all five lines resemble absorption line shapes. The broadening of the weakest line, no. 5 ($g_{\text{eff}} = 1.3$), was so great that the line apparently disappeared after heating at 800 °C for 90 h (spectrum b in Fig. 1). This line is, in fact, particularly sensitive to the angular dependence on the orientation of the crystal with respect to **B** and, therefore, additionally broadened.

Unfortunately, X-ray diffraction data and EPR spectra could not be obtained from the same heat-treated crystals since it was important that the shape of the crystals used to collect the spectra should remain unchanged over a complete heating series. Table 1 lists the lattice constants determined from powders of crystal fragments heated in independent experiments carried out under the same conditions as used for EPR. However, sample no. 4 of Table 1 refers to the crystal used for the 800 °C EPR series; lattice parameters were obtained from a fragment of the crystal after the last anneal (186 h).

From the lattice constants (Table 1), Al and Si site occupancies may be calculated for the T positions (Table 2) using the approach of Kroll and Ribbe (1987).

DISCUSSION

The five fine-structure lines in the albite spectrum are attributed to Fe³⁺ at one crystallographic position. A unique assignment to one of the four nonequivalent T positions in albite cannot be made on the basis of the spectra alone, however, since all four T positions are general positions without symmetry. Instead, the assignment is possible based on geometrical and crystal-chemical arguments. Generally Fe³⁺ shows a somewhat larger radius than Al³⁺ in oxides and commonly substitutes for Al³⁺ in silicates. The AlO₄ tetrahedron of position T1(O) in low albite exhibits the largest volume of the four distinct tetrahedra. No additional Fe³⁺ signals were found that could be assigned to T positions other than T1(O). The assignment of the five Fe³⁺ fine-structure lines to T1(O) is out of the question. A complete substitution of Fe³⁺ for Al³⁺ has been demonstrated in potassium feldspar by Wones and Appleman (1961), who synthesized iron sanidine KFeSi₃O₈.

Semiquantitative descriptions of the observed changes of line shape depending on the heat treatment can be given in terms of two ratios, $^{\Delta B}R_n$ and hR_n . The ratio $^{\Delta B}R_n$ is defined as

$$^{\Delta B}R_n = \Delta B_T / \Delta B_0, \quad (1)$$

where ΔB designates the experimental line width (cf. Fig. 2) and the subscript n is the line number (mainly lines 1, 2, and 3). The subscripts T and 0 refer to the temperature of the heat-treated and unheated states, respectively. Similarly,

$$^hR_n = h_T / h_0, \quad (2)$$

where h designates the height of the signal (cf. Fig. 2). Equations 1 and 2 simply measure the respective increase or decrease of width ΔB and signal height h with increasing heating time at constant temperature. Figure 2 illus-

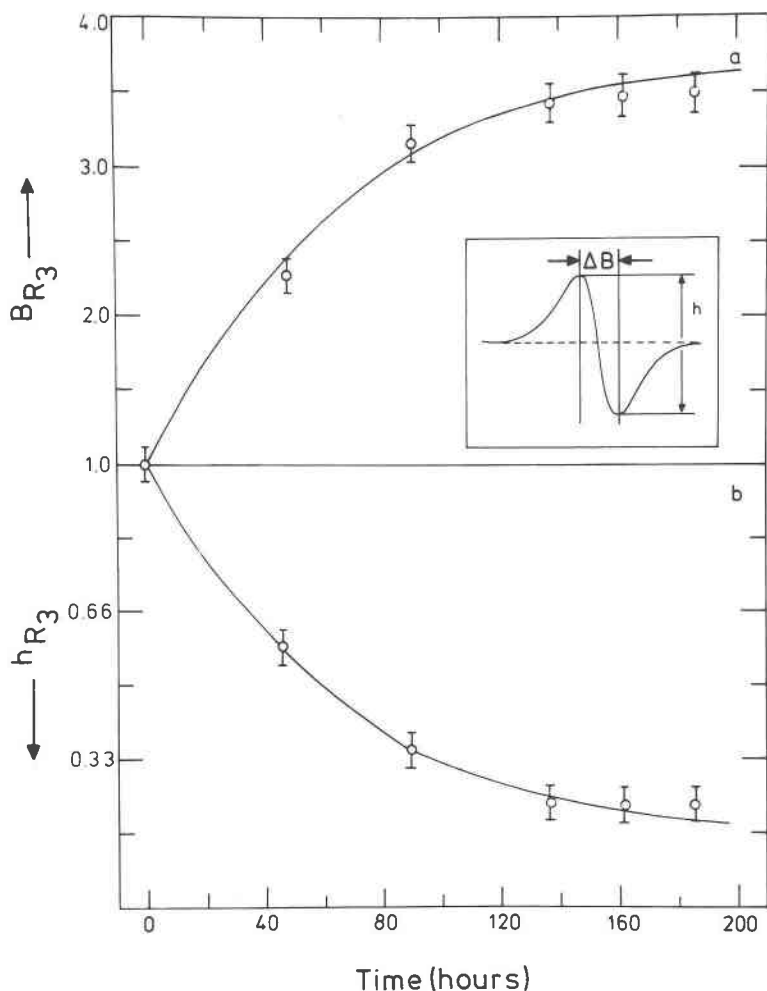


Fig. 2. (a) Ratio $\Delta^B R_3$ of the observed EPR line width ΔB , $\Delta^B R_3 = \Delta B_T / \Delta B_0$. Subscripts T and 0 refer to the temperature of heating ($T = 800$ °C) and the unheated state, respectively; subscript 3 refers to the line number (Fig. 1). For the unheated crystal, $\Delta^B R_n = 1$; after treatment, generally $\Delta^B R_n > 1$. (b) Ratio ${}^h R_3$ of the observed line amplitudes h , ${}^h R_3 = h_T / h_0$, where h is the peak-to-peak height (amplitude) and $T = 800$ °C.

trates the increase in line width ($\Delta^B R_n$) and decrease in height (${}^h R_n$) with time for the crystal heated at 800 °C. It should be noted that no shifts of the center positions of the signals were observed and the values of g_{eff} remained constant. This is taken to indicate that the occupancy of Fe³⁺ in T1(O) remained unchanged over the range of temperatures and times investigated. The Fe³⁺ ions remained at their sites.

The natural width of an EPR line is determined by the Heisenberg uncertainty principle, i.e., the lifetime Δt of the excited state of the spin system:

$$\Delta t \Delta E \geq h/2\pi,$$

i.e.,

$$g\beta\Delta B\Delta t \geq h/2\pi, \quad (3)$$

where ΔE is the uncertainty (standard deviation) in our measurement of the energy of the system, ΔB is the line

width due to the uncertainty of the energy, g is the electronic g factor, β is the Bohr magneton, and h is Planck's constant. In our case, $\Delta t \Delta B \geq (11.4 \times 10^{-8})/g \text{ G}\cdot\text{s}$. If $g = 2$, 9.5 GHz (X-band) corresponds to 3.4 kG; i.e., when the lifetime of the state is, e.g., 60×10^{-9} s, the broadening of the line is of the order of 1 G. The observed line widths ($\Delta B \approx 50$ G) are much too broad to represent the "natural" width, however. In general a number of factors could contribute to additional line broadening, including (1) saturation of the spin system, (2) inhomogeneity of \mathbf{B} over the volume of the crystal, (3) spin-spin interaction (e.g., between adjacent Fe³⁺ ions), (4) unresolved hyperfine and superhyperfine interactions, (5) spin-lattice relaxation, (6) defects such as linear and planar displacements in the crystal and possible domain structures, and (7) natural disorder at positions adjacent to the Fe³⁺ center.

In order to minimize the effects of factor 1, spectra

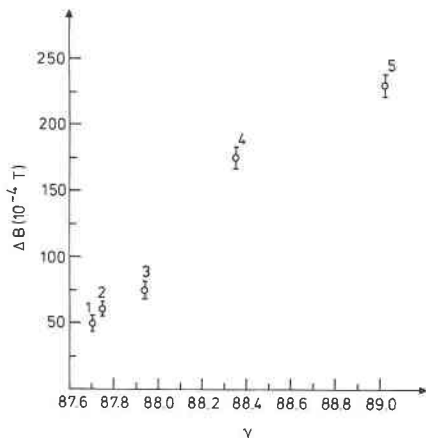


Fig. 3. Width ΔB , of line 3 (cf. Fig. 1) as a function of the lattice angle γ . No. 1, natural albite from Amelia. No. 2, crystal heated at 700 °C, 1 kbar, 144 h. No. 3, crystal heated at 800 °C, 1 kbar, 24 h. No. 4, crystal heated at 800 °C, 1 kbar, 186 h. No. 5, crystal heated at 850 °C, 0.5 kbar, 120 h. A different crystal was used for each heating experiment.

were taken using different microwave powers, and the dependence of line width on intensity was tested. In any case, spectra obtained for the 800 °C series of heated crystals were collected under identical conditions. The homogeneity of \mathbf{B} (factor 2) over the crystal volume was tested using NMR of H⁺.

Factor 3 may be neglected in view of the small concentration of Fe³⁺ in Amelia albite. The shortest distance between two adjacent T1(O) sites is ~ 7.5 Å. If a paramagnetic ion is located at an adjacent T site other than T1(O), that distance is reduced to ~ 2.6 Å, but the statistical probability of formation of Fe³⁺ pairs is still exceedingly small since lines of paramagnetically isolated Fe³⁺ at T1(m), T2(O), and/or T2(m) could not be detected, either before or after the heat treatments. If it is assumed that 0.01–0.03 Fe³⁺ ions are present per unit cell, as in the case of our albite, the observed increase of line width ΔB cannot be due to spin-spin interaction among adjacent T sites. Factors 4 and 5 may contribute, in principle, to ΔB in albite, but it is assumed that they do not depend critically on heat treatment. With respect to factor 6, optical inspection of the single crystals did not reveal any mechanical defects after hydrothermal heating. Moreover, the X-ray diffraction patterns did not show evidence of any domain structure induced by heating. The widths of the diffraction lines of the heated samples remained as sharp as those of the unheated crystal, also after heat treatment at 850 °C.

It is concluded that factor 7 is the dominant one in line broadening. We interpret the increase of ΔB and the change of line shape as being due to increasing local Al,Si disorder around the Fe³⁺ sites that perturbs the crystal field at the Fe³⁺ center. Small variations in the local environment of the Fe³⁺ site cause a range of different crystalline electric fields and produce deviations in the ori-

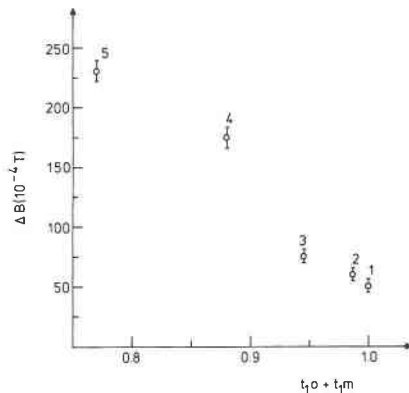


Fig. 4. Variation of line width of signal 3, ΔB_3 , with the values of $t_{1,o} + t_{1,m}$. The numbers 1 to 5 refer to the samples and heat treatments specified in Table 1.

entation of the principal axes of the \mathbf{g} tensor (Scala et al., 1978; Matyash et al., 1981; Petrov and Hafner, 1988). Well-ordered natural albite and microcline show line widths not smaller than about 50 G whereas partially ordered adularia and orthoclase and disordered sanidine exhibit widths of 150–350 G (Marfunin et al., 1967), depending on the particular orientation (Petrov and Hafner, 1988).

The parameters ΔB , ${}^{\Delta}R_n$, and hR_n appear to be quite sensitive to the degree of Al,Si disorder, but especially when the degree of order is still high. The linear relationship between ΔB and the lattice angle γ (cf. Fig. 3) is related to a linear decrease in the difference in Al occupancy at T1(O) and T1(m) apparently as long as the crystals are still predominantly ordered. Tables 1 and 2 indicate that the lattice constants and site occupancies changed significantly in our experiments depending on the heating conditions, though the crystals remained predominantly ordered. The dependence of the sum of site occupancies $t_{1,o} + t_{1,m}$ of Al at T1(O) and T1(m) on ΔB is shown in Figure 4. It should be noted that ΔB , as well as the lattice constants, depends on the geometrical degree of disorder over the T sites, independent of the temperature and time relationship by which the degree of disorder was attained.

Al,Si disorder is most probably not the only consequence of the heat treatments. It was observed that after heating at about 800 °C for 90 h, a very broad line near $g = 2$ appeared. This became broader and more intense after heating at still higher temperatures and/or over longer periods of time (cf. spectrum b in Fig. 1). Small contributions from the line near $g = 2$ are already present in the spectra from crystals heated below 800 °C and can just be detected in unheated crystals (spectrum a of Fig. 1). This line may be due to the presence of very small amounts of iron oxide particles and/or to clusters of defects at interstitial positions in the natural albite that increase in abundance with heat treatment. Cluster formation during heat treatment may be coupled with the destruction of hydroxyl groups substituted for oxygen at

the anion positions (Smith, 1974). Hints at this had been given already by Donnay et al. (1959). At temperatures higher than about 900 °C, the line near $g = 2$ becomes so broad that it almost covers the lines of Fe³⁺ substituted at T1(O).

The line broadening could be associated with diffusion of Na⁺, Ca²⁺, and other cations or vacancies at the M positions, possibly coupled with diffusion of OH⁻. However, the amount of Ca²⁺ is small in our albite, and the self-diffusion coefficient of Na⁺ is such that significant Na⁺ exchange among M sites occurs below 595 °C (Bailey, 1971), i.e., well below the temperatures of the beginning of line broadening (>700 °C). If Na⁺ diffusion is the initiating mechanism for possible exchange of other cations or defects at M sites, line broadening is expected to begin at lower temperatures than observed. The linear correlation between the lattice constants and ΔB is indicative that broadening of ΔB results primarily from Al,Si exchange among the T sites (factor 7, above). It is well known that lattice parameters such as α , γ , and b , c linearly depend on site occupancies $t_{1,0} - t_{1,m}$ and $t_{1,0} + t_{1,m}$, respectively, over the full range of structural states.

Experiments on sanidine showed that heating at 1050 °C (i.e., at temperatures just below the melting point) for times of more than 360 h is necessary to produce sufficient exchange of Fe³⁺ between the T1 and T2 sites to be detected in EPR spectra (Petrov and Hafner, 1988). The present EPR results on albite are indicative of a similarly slow exchange mechanism for Fe³⁺.

CONCLUSIONS

(1) Heat treatment of Amelia albite up to a temperature of 500 °C for at least 7 d did not cause changes in X-band EPR spectra. However, heating between 700 and 850 °C produced systematic broadening of the Fe³⁺ lines that could be correlated with changes in the lattice constants. The broadening is attributed to increasing Al,Si disorder in crystals that are still predominantly ordered.

(2) A change in the g values of the Fe³⁺ lines could not be detected, Fe³⁺ remaining located at T1(O) until at least 850 °C.

(3) Fe³⁺ exchange among T sites appears to be as slow in ordered albite as it is in disordered sanidine.

ACKNOWLEDGMENTS

We thank K. Schürmann, University of Marburg, for hydrothermal heating, R. M. Mineeva, IGEM of the Academy of Sciences of the USSR, Moscow, for valuable discussion, and Mrs. I. Schmiemann for the determination of lattice parameters from X-ray powder-diffraction patterns.

REFERENCES CITED

Bailey, A. (1971) Comparison of low-temperature with high-temperature diffusion of sodium in albite. *Geochimica et Cosmochimica Acta*, 35, 1073-1081.

- Bambauer, H.U., Eberhard, E., and Viswanathan, K. (1967) The lattice constants and related parameters of "plagioclases (low)." *Schweizerische Mineralogische und Petrographische Mitteilungen*, 47, 351-364.
- Bart, J.C.J., Burriesci, N., Cariati, F., Cavallaro, S., Giordano, N., and Petrer, M. (1982) Nature and distribution of iron in volcanic glass: Mössbauer and EPR study of lipari pumice. *Bulletin de la Société Française de Minéralogie et de Cristallographie*, 105, 43-50.
- Burnham, C.W. (1962) IBM computer program for least-squares refinement of crystallographic lattice constants. *Carnegie Institution of Washington Year Book* 61, 132-135.
- Calas, G., and Petiau, J. (1983) Structure of oxide glasses: Spectroscopic studies of local order and crystallochemistry. *Geochemical implications*. *Bulletin de la Société Française de Minéralogie et de Cristallographie*, 106, 33-55.
- Deer, W.A., Howie, R.A., and Zussman, J. (1963) *Rock-forming minerals*, vol. 4, framework silicates, p. 110. William Clowes and Sons, London.
- Donnay, G., Wyart, J., and Sabatier, G. (1959) Structural mechanism of thermal and compositional transformations in silicates. *Zeitschrift für Kristallographie*, 112, 161-168.
- Friebele, E.J., Wilson, L.K., Dozier, A.W., and Kinser, D.L. (1971) Antiferromagnetism in an oxide semiconducting glass. *Physica Status Solidi (b)*, 45, 323-331.
- Fu, Y., Bershov, L.V., Petrov, I., and Hafner, S.S. (1987) Distribution and exchange kinetics of ferric iron over the tetrahedral positions in potassium and sodium feldspar. *Terra Cognita*, 7, 388.
- Gaite, J.M., and Michoulier, J. (1970) Application de la résonance paramagnétique électronique de l'ion Fe³⁺ à l'étude de la structure des feldspaths. *Bulletin de la Société Française de Minéralogie et de Cristallographie*, 93, 341-356.
- Griscom, D.L. (1980) Electron spin resonance in glasses. *Journal of Non-Crystalline Solids*, 40, 211-272.
- Kroll, H., and Ribbe, P.H. (1987) Determining (Al,Si) distribution and strain in alkali feldspars using lattice parameters and diffraction-peak positions: A review. *American Mineralogist*, 72, 491-506.
- Kroll, H., Schmiemann, I., and von Cölln, G. (1986) Feldspar solid solutions. *American Mineralogist*, 71, 1-16.
- Marfunin, A.S., Bershov, L.V., Meilman, M.L., and Michoulier, J. (1967) Paramagnetic resonance of Fe³⁺ in some feldspars. *Schweizerische Mineralogische und Petrographische Mitteilungen*, 47, 13-20.
- Matyash, V.I., Bagmut, N.N., Litovchenko, C.A., and Proshko, Ya.V. (1981) Anwendung der EPR-Daten von Fe³⁺ zur Bestimmung von Strukturbesonderheiten der Alkalifeldspäte. *Mineralogicheskii Zhurnal*, 3, 76-80.
- Michoulier, J., and Gaite, J.M. (1972) Site assignment of Fe³⁺ in low symmetry crystals. Application to NaAlSi₃O₈. *Journal of Chemical Physics*, 56, 5205-5213.
- Mineeva, R.M., Bershov, L.V., Marfunin, A.S., Fieldmann, V.I., and Speranskii, A.V. (1984) Strukturformen von Eisen und Mangan in Tektiten und Impaktiten nach EPR-Daten. *Mineralogicheskii Zhurnal*, 2, 30-35.
- Petrov, I., and Hafner, S.S. (1988) Location of trace Fe³⁺ ions in sanidine KAlSi₃O₈. *American Mineralogist*, 73, 97-104.
- Scala, C.M., Hutton, D.R., and McLaren, A.C. (1978) NMR and EPR studies of the chemically intermediate plagioclase feldspars. *Physics and Chemistry of Minerals*, 3, 33-44.
- Smith, J.V. (1974) *Feldspar minerals*, Vol II. Chemical and textural properties, p. 7. Springer-Verlag, Berlin.
- Wones, D.R., and Appleman, D.E. (1961) X-ray crystallography and optical properties of synthetic monoclinic KFeSi₃O₈ iron-sanidine. U.S. Geological Survey Professional Paper 424-C, C309-C310.

MANUSCRIPT RECEIVED APRIL 14, 1988

MANUSCRIPT ACCEPTED JANUARY 3, 1989